Dependence of nanoscale heat transfer across a closing gap on the substrate material and ambient humidity

Qilong Cheng,[1, a)] Siddhesh Sakhalkar,[1] Amin Ghafari,[1] Yuan Ma,[2] and David Bogy[1]
[1)] *University of California at Berkeley, Berkeley, California 94720, USA.*
[2)] *Texas A&M University, College Station, Texas 77843, USA.*

(Dated: 4 May 2020)

We investigate the heat transfer across a closing nanoscale gap between an operational microelectronic device and a static substrate in ambient conditions. The device contains an embedded micro-heater and a nanoscale metal wire that works as a thermometer. The heater causes a microscale protrusion by thermal expansion such that its surface approaches the substrate until contact occurs. Meanwhile, the metal wire located near the center of the protrusion surface measures the temperature of the protrusion, which is dependent on the size of the gap, the substrate material and the ambient conditions. We study the nanoscale heat transfer using three different substrates and find that their thermal conductivity plays an essential role. Finally, the experiments are conducted under different relative humidity (RH) conditions. The results show that the ambient humidity can also affect the nanoscale heat transfer when RH > 75%.

Heat transfer between two bodies at different temperatures is a broadly studied topic.[1–6] As the microelectronics industry pushes the physical size of elements in the devices down to nanoscale dimensions, the nanoscale heat transfer leads to mass transfer problem that affects the efficiency of the devices and introduces reliability issues.[7,8] Therefore, understanding the nanoscale heat transfer and its tunability becomes crucial.

In our previous studies, we have performed the nanoscale heat transfer experiments between two bodies across a closing gap with good agreement achieved between the experiments and modelling based on van der Waals (vdW) force driven phonon conduction theory.[5,9–13] In this paper, we focus on studying the nanoscale heat transfer using different substrate materials and relative humidity (RH) conditions. To simplify the participators that the nanoscale heat transfer is dependent on, three substrates with various thermal properties (silicon/GaAs/glass wafers) are chosen instead of the multilayered media that are broadly used in the industry. The experimental results show that the substrate material and the ambient humidity can significantly affect the nanoscale heat transfer.

In the experiments, we investigate the nanoscale heat transfer across a closing initial nanoscale gap between an operational microelectronic device and a substrate in ambient conditions. This device is a perpendicular magnetic recording (PMR) head that contains a well-understood embedded micro-heater[14] and a metal wire with width around 100 nm, as shown in Fig. 1. In magnetic recording hard disk drives, the micro-heater is used to adjust the spacing between the recording head and a rotating disk. The nanoscale metal wire, also known as embedded contact sensor (ECS), is located near the transducer elements and is typically used to detect head-disk contact.[15–17] In this study, the metal wire works as a resistance based thermometer that has a constant temperature coefficient of resistance (TCR) of 0.003/K, which is determined by calibration experiments using a 4-probe measurement. In the experiments, the resistance change of the metal wire is used to measure the temper-

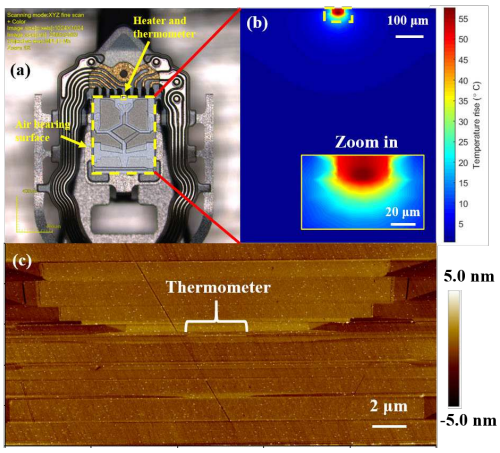

FIG. 1. A diagram of the perpendicular magnetic recording (PMR) recording head showing (a) the under side of the air bearing surface (ABS); (b) the simulated temperature field at the device surface when the heater power is 80 mW and the device-substrate gap is around 2 nm; (c) the AFM image of the device surface where the metal wire (thermometer) is located at the center and surrounded by metal shields and other elements such as the writer and reader (Ni, Fe, Cu).

[a)] Email: qlcheng@berkeley.edu

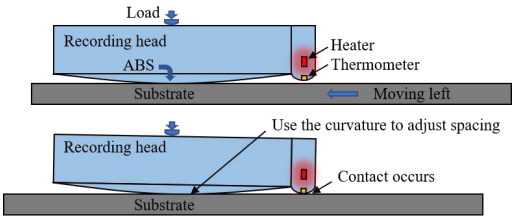

FIG. 2. A schematic diagram (not to scale) of the experimental setup. The curvature of the air-bearing surface is used to adjust the initial spacing between the thermometer and the substrate. Direct contact can also be realized.

ature rise due to the micro-heater by:

$$R(T) = R(T_0)(1 + \alpha(T - T_0)), \quad (1)$$

where $R(T)$ and $R(T_0)$ are the resistances of the metal wire at any temperature T and room temperature T_0 and α is the TCR. The metal wire is biased using a small enough DC voltage for its overall self-heating to be ignored (~ 0.1 °C rise). The resolution of the thermometer is ~ 0.1 °C, which is estimated from the resolution of resistance measurement $\sim 0.02\ \Omega$. Figs. 1(b) and 1(c) show that the temperature field near the metal wire is uniform since the micro-heater has a microscale heated area. Thus, the metal wire can measure the temperature of the device surface accurately. Therefore, this device provides an excellent tool for conducting such experiments as the nanoscale heat transfer between two bodies. See the supplementary material, section S1, for the calibration details of the thermometer.

The experimental setup is shown in Fig. 2. The ABS of the device is loaded onto a substrate. The substrate is fixed on a metal heat sink, so the bottom surface of the substrate is kept at room temperature. Then the heater heats the device and a microscale protrusion is formed on its surface. Thus, the gap between the surface of the device and the substrate decreases with the heater power until they are in contact with each other. Meanwhile, the thermometer located at the center of the protrusion surface measures the protrusion temperature as it approaches the substrate. Fig. 2 also shows that the initial gap between the two bodies can be adjusted by the movement of the substrate. For example, when the substrate moves left, the friction between the crowned ABS and the substrate forces the device to tilt and hence the gap size is decreased. Even direct contact can be realized as an initial condition.

Fig. 3 shows the measured temperature rise as a function of the heater power using three different substrates (silicon/GaAs/glass wafers, surface roughness $S_q \sim 0.1$ nm). The solid lines present the results of cases for which the initial gap size is around 21.3 nm (from simulation as shown in Fig. 4) while the dashed lines are the cases of direct contact as the initial condition. The measured temperatures firstly increase linearly with the heater power where the air conduction across the gap dominates to almost 2 nm. Then with the decrease of the spacing, enhanced phonon conduction heat transfer dominates and causes a drop in the temperature. Finally the device protrusion makes contact with the substrate and a much smaller heating slope is observed due to contact heat conduction. Fig. 4 shows that the enhanced phonon conduction heat transfer begins to take effect when the spacing is within around 2 nm, which is close to the prediction of another approach using an atomic formalism.[18] The detailed description of the simulation model used to determine the temperature and spacing fields in Figs. 1(b) and 4 can be found in Ref. 12.

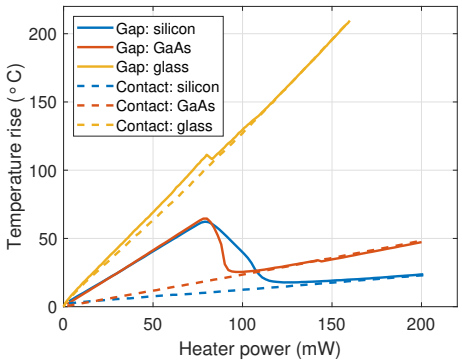

FIG. 3. The temperature rise as a function of the heater power in the case of an open gap or direct contact on silicon/GaAs/glass wafers under the condition of indoor humidity around 35%.

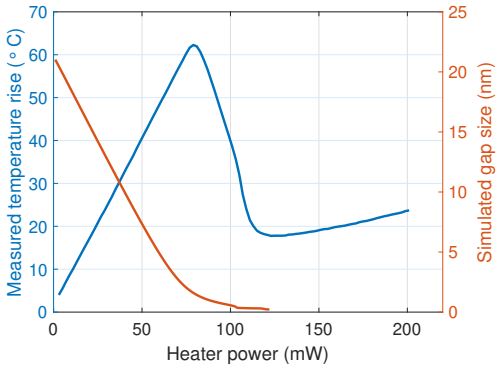

FIG. 4. The measured temperature rise and the simulated gap size versus the heater power for the case of silicon wafer.

Comparing the cases of 21.3 nm initial gap (solid lines) and the cases of initial direct contact (dashed lines), we see that the contact parts of the curves with 21.3 nm gap overlap with the dashed lines. Comparing among the three substrate materials, we find that the material thermal conductivity plays an important role. The thermal conductivities of the substrates are listed in Table I. During the first linear part of each curve, the glass curve has the largest heating slope because the glass has the smallest thermal conductivity (1.3 W/mK) and hence the glass substrate undergoes a higher temperature rise compared to silicon and GaAs substrates (148 W/mK and 56 W/mK). See the supplementary material, section S2, for the simulation results of substrate temperature rise. After contact occurs, the slope is determined by the thermal conductivity of the substrate. The heating slope becomes smaller since the contact heat conduction becomes stronger when using a better thermal conductor such as silicon. Therefore, the temperature drop is essentially dependent on the material thermal conductivity. The steepness of the drop depends on the vdW forces and the heat transfer coefficient of the phonon conduction across the gap. The vdW force between the device surface and the substrate causes a steeper drop in the curve of the temperature rise versus the heater power, as demonstrated in Ref. 12. The heat transfer coefficient affects the heater power required to fill the last 2 nm of the gap until contact.

TABLE I. Thermal conductivity of the substrates

Substrate	Thermal conductivity (W/mK)
Silicon	148
GaAs	56
Glass	1.3

Next we study the effect of the RH conditions on the nanoscale heat transfer. The humidity is controlled as shown in Fig. 5. The entire experimental setup is put into a sealed chamber with a dry air inlet and a vacuum pump, which are used to achieve low humidity conditions. For higher RH, different types of saturated salt solutions (NaCl, KNO_3, K_2SO_4, etc.) or pure water are put into the chamber to keep the relative humidity at different values.[19] The experiments are conducted after the humidity reaches equilibrium in the chamber ($\sim$ 10 h). We note that the pressure inside the chamber is always 1 atm.

Fig. 6 shows the results of the humidity experiments using a silicon substrate. The case of direct contact on silicon which is independent of humidity is also added in Fig. 6 for comparison. Fig. 6 shows no change in the measurement when RH $\leq$ 75%. When the RH $>$ 75% , the curves of the temperature rise versus the heater power show a smaller temperature rise and a more gradual temperature drop. The last linear parts of all curves, namely the contact parts, also overlap with the black dashed line, which is measured for the case of direct contact. Thus we have shown that the nanoscale heat transfer depends on the ambient humidity for RH $>$ 75%.

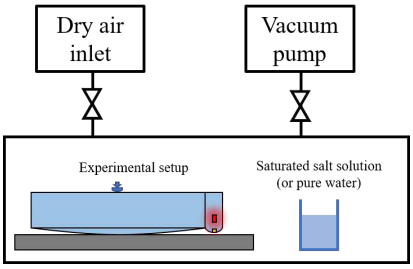

FIG. 5. A diagram showing how the humidity in the sealed chamber is controlled.

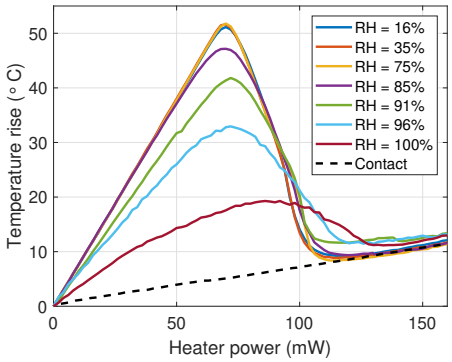

FIG. 6. The temperature rise as a function of the heater power under different RH conditions with the substrate of silicon.

Fig. 6 shows that the nanoscale heat transfer is enhanced when the humidity is beyond 75%. One of the potential explanations is that a thin water layer is formed under high humidity conditions.[20] The water layer reduces the spacing between the device protrusion and the substrate and absorbs a portion of heat. A previous study shows that the thickness of the absorbed water layer remains smaller than 1 nm when RH is low and increases to 3 nm under high RH.[21] The trend matches the results in Fig. 6 in that the water layer takes effect when its thickness is comparable to the spacing, namely under high humidity conditions. See the supplementary material, section S3, for the transient measurement of the temperature rise when the heater power is 70 mW. At this power, the gap size is a little larger than 2 nm (Fig. 4), but the transient plot of 100% RH shows that the water layer fills the gap and the heater is heating the layer continuously, resulting in the lower temperature at the thermometer. Therefore, the interaction between

the water layer and the spacing accounts for the smaller temperature rise when the RH increases. The more gradual temperature drop can also be explained by the water layer because the water layer has a larger heat capacity and hence acts as a buffer.

In conclusion, the nanoscale heat transfer experiments between two bodies at different temperatures are conducted using different substrates or under different RH conditions. The results show that the nanoscale heat transfer becomes stronger when a substrate material with larger thermal conductivity is used or when the humidity is higher than 75%. Therefore, the substrate material and the ambient humidity are both important participators for studying the nanoscale heat transfer across a closing gap, which in turn can be used to modulate the nanoscale heat transfer.

See the supplementary material S1 for the calibration details of the thermometer, S2 for the simulation results of the substrate temperature rise, and S3 for the transient measurement in the humidity experiments.

The data that support the findings of this study are available from the corresponding author upon reasonable request. The work was supported by the Computer Mechanics Laboratory at University of California at Berkeley. We thank Western Digital Corporation for supplying the components.

[1]S. Shen, A. Narayanaswamy, and G. Chen, "Surface phonon polaritons mediated energy transfer between nanoscale gaps," Nano letters **9**, 2909–2913 (2009).
[2]K. Kim, B. Song, V. Fernández-Hurtado, W. Lee, W. Jeong, L. Cui, D. Thompson, J. Feist, M. H. Reid, F. J. García-Vidal, *et al.*, "Radiative heat transfer in the extreme near field," Nature **528**, 387 (2015).
[3]B. Song, D. Thompson, A. Fiorino, Y. Ganjeh, P. Reddy, and E. Meyhofer, "Radiative heat conductances between dielectric and metallic parallel plates with nanoscale gaps," Nature nanotechnology **11**, 509 (2016).
[4]B. V. Budaev, A. Ghafari, and D. B. Bogy, "Intense radiative heat transport across a nano-scale gap," Journal of Applied Physics **119**, 144501 (2016).
[5]Y. Ma, A. Ghafari, B. Budaev, and D. Bogy, "Controlled heat flux measurement across a closing nanoscale gap and its comparison to theory," Applied Physics Letters **108**, 213105 (2016).
[6]B. V. Budaev and D. B. Bogy, "Systems with a constant heat flux with applications to radiative heat transport across nanoscale gaps and layers," Zeitschrift für angewandte Mathematik und Physik **69**, 71 (2018).
[7]M. H. Kryder, E. C. Gage, T. W. McDaniel, W. A. Challener, R. E. Rottmayer, G. Ju, Y.-T. Hsia, and M. F. Erden, "Heat assisted magnetic recording," Proceedings of the IEEE **96**, 1810–1835 (2008).
[8]S. V. Sakhalkar and D. B. Bogy, "Effect of rheology and slip on lubricant deformation and disk-to-head transfer during heat-assisted magnetic recording (hamr)," Tribology Letters **66**, 145 (2018).
[9]B. V. Budaev and D. B. Bogy, "Computation of radiative heat transport across a nanoscale vacuum gap," Applied Physics Letters **104**, 061109 (2014).
[10]B. V. Budaev and D. B. Bogy, "Heat transport by phonon tunneling across layered structures used in heat assisted magnetic recording," Journal of Applied Physics **117**, 104512 (2015).
[11]Y. Ma, A. Ghafari, B. V. Budaev, and D. B. Bogy, "Measurement and simulation of nanoscale gap heat transfer using a read/write head with a contact sensor," IEEE Transactions on Magnetics **53**, 1–5 (2016).
[12]S. Sakhalkar, Q. Cheng, A. Ghafari, Y. Ma, and D. Bogy, "Numerical and experimental investigation of heat transfer across a nanoscale gap between a magnetic recording head and various media," Applied Physics Letters **115**, 223102 (2019).
[13]Y. Ma, A. Ghafari, Y. Wu, and D. Bogy, "A study of the nanoscale heat transfer in the hdd head–disk interface based on a static touchdown experiment," IEEE Transactions on Magnetics **56**, 1–7 (2020).
[14]J. Zheng, *Dynamics and stability of thermal flying-height control sliders in hard disk drives*, Ph.D. thesis, UC Berkeley (2012).
[15]J. Xu, Y. Shimizu, M. Furukawa, J. Li, Y. Sano, T. Shiramatsu, Y. Aoki, H. Matsumoto, K. Kuroki, and H. Kohira, "Contact/clearance sensor for hdi subnanometer regime," IEEE transactions on magnetics **50**, 114–118 (2014).
[16]H. Wu, S. Xiong, S. Canchi, E. Schreck, and D. Bogy, "Nanoscale heat transfer in the head-disk interface for heat assisted magnetic recording," Applied Physics Letters **108**, 093106 (2016).
[17]H. Wu and D. Bogy, "Use of an embedded contact sensor to study nanoscale heat transfer in heat assisted magnetic recording," Applied Physics Letters **110**, 033104 (2017).
[18]V. Chiloyan, J. Garg, K. Esfarjani, and G. Chen, "Transition from near-field thermal radiation to phonon heat conduction at sub-nanometre gaps," Nature communications **6**, 6755 (2015).
[19]F. O'brien, "The control of humidity by saturated salt solutions," Journal of Scientific Instruments **25**, 73 (1948).
[20]Q. Cheng, Y. Ma, and D. Bogy, "Effect of humidity on the nanoscale heat transfer at the head-media interface," in *ASME 2019 28th Conference on Information Storage and Processing Systems* (American Society of Mechanical Engineers Digital Collection).
[21]D. B. Asay and S. H. Kim, "Effects of adsorbed water layer structure on adhesion force of silicon oxide nanoasperity contact in humid ambient," The Journal of chemical physics **124**, 174712 (2006).